Effect of uniaxial stress on solid phase epitaxy in patterned Si wafers

N. G. Rudawski,[a] K. N. Siebein, and K. S. Jones
Department of Materials Science and Engineering, University of Florida, Gainesville, Florida 32611-6400

(Received 26 May 2006; accepted 30 June 2006; published online 25 August 2006)

The effect of uniaxial stress on solid phase epitaxy in patterned {001} Si wafers after ion implantation and annealing was investigated. It was found that mask edge defect formation was suppressed when tensile stresses greater than 100 MPa were applied along the ⟨110⟩ direction. The application of compressive stress retarded ⟨001⟩ regrowth up to ~6% and enhanced ⟨110⟩ regrowth up to ~6%, while tensile stress enhanced ⟨001⟩ regrowth up to ~60% and retarded ⟨110⟩ regrowth up to ~40%. A stress-dependent regrowth velocity model qualitatively agrees with the observed trends in the ratio of ⟨001⟩ and ⟨110⟩ regrowth velocities. © *2006 American Institute of Physics*. [DOI: 10.1063/1.2337994]

The suppression of mask edge defects during solid phase epitaxy (SPE) of two-dimensional amorphous (α) Si is of key importance in the formation of shallower, more active junctions. The evolution of these defects in the form of dislocation half loops and arrays of stacking faults forming on {111} planes at the ⟨110⟩/⟨001⟩ α/crystalline interface during SPE has been previously reported.[1,2] However, by reducing regrowth velocity of the ⟨110⟩ interface and enhancing the regrowth velocity of the ⟨001⟩ interface, the formation of these defects can be suppressed.[3,4] Ross and Jones showed that the use of Si_3N_4 patterning with thickness of 150 nm provided a tensile stress (σ) in the ⟨110⟩ direction large enough to suppress defect formation.[3] Likewise, Olson *et al.* revealed that ⟨110⟩ tensile stresses appeared to influence the geometry of the regrowing interface so as to prevent mask edge defect formation.[4] It is known that regrowth velocity can be controlled by the application of different stress states.[5–8] For example, uniaxial bending stress applied in the plane of a ⟨001⟩ regrowing interface slightly altered regrowth velocity with tensile or compressive stress enhancing or retarding SPE, respectively.[5,6] In comparison, others showed that the application of hydrostatic pressure exponentially enhanced ⟨001⟩ regrowth velocity.[7,8] Shin *et al.* revealed that the use of SiO_2 films to induce a compressive stress at annealing temperature accelerated the formation of {111} stacking fault arrays in two-dimensional structures.[9,10] In this experiment, the use of uniaxial bending stress to control regrowth velocity of the interfaces in two-dimensional α-Si was studied in an effort to control defect formation.

In this study, 150 nm of Si_3N_4 and 10 nm of SiO_2 were deposited on {001} oriented 750 μm Si wafers and patterned to create lines and square openings with approximate dimensions of 0.1–0.3 μm. Si^+ implantation at energies of 20 and 60 keV with doses of 1×10^{15} cm^{-2} produced an α-Si layer ~120 nm deep with rounded corners beneath mask edges, as shown in Fig. 1(a). The wafers were cleaved into rectangular bars along ⟨110⟩ directions with approximate dimensions of 0.5×6.0 cm^2. The Si_3N_4/SiO_2 mask was removed prior to annealing by etching with a 49% HF solution for 30 min, and the samples were annealed under stress at 500 °C between 1 and 3 h. and A novel quartz bending apparatus was used to induce a four-point bend in the Si pieces generating uniaxial stress along the ⟨110⟩ direction. The analysis used to calculate the maximum stress in the wafer is described elsewhere.[4] Furthermore, it was determined that the stress gradient in the sample between in- and outbending points was linear to a good approximation. Tensile and compressive stresses were studied up to a stress magnitude of ~200 MPa. Cross-sectional transmission electron microscopy (XTEM) was used to image the regrowth of α-Si layers and the evolution of mask edge defects at different times during recrystallization. For each stress, the ⟨001⟩ regrowth velocity $v_{\langle001\rangle}$ was calculated by measuring the α-Si regrowth from the end of range (EOR) damage at the center of the implant profile, while the ⟨110⟩ regrowth velocity $v_{\langle110\rangle}$ was calculated by measuring the α-Si regrowth from the EOR damage at a depth of 25 nm at different annealing times. Additionally, the evolution of the ⟨110⟩/⟨001⟩ interface angle θ as a function of applied stress was investigated. The parameters $v_{\langle001\rangle}$, $v_{\langle110\rangle}$, and θ are displayed schematically in Fig. 1(b).

Figures 2(a)–2(c) show XTEM images of samples annealed without stress up to 3 h at different time intervals. After 1 h of annealing, the rounded corner of the as-implanted profile has started to disappear and the corner begins to appear square in nature, as shown in Fig. 2(a). After 2 h of annealing, shown in Fig. 2(b), the corner has become quite sharp, though no meeting of the two regrowth interfaces has occurred. However, by the time 3 h of annealing has occurred, the two interfaces have met and "pinch-off" has occurred, thus forming mask edge defects, as shown in Fig. 2(c). Plots of θ versus stress for 1 and 2 h annealing

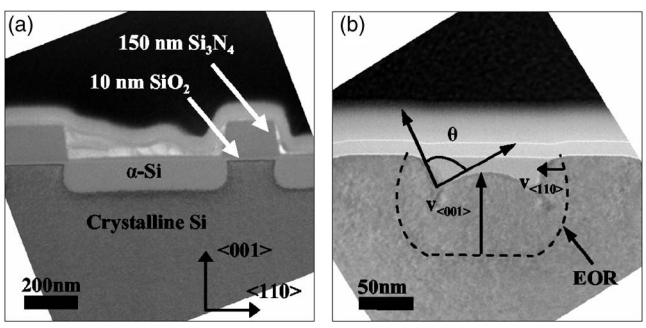

FIG. 1. XTEM micrographs of (a) an as-implanted structure and (b) schematic representations of the parameters θ, $v_{\langle001\rangle}$, and $v_{\langle110\rangle}$.

[a]Author to whom correspondence should be addressed; electronic mail: ngr@ufl.edu

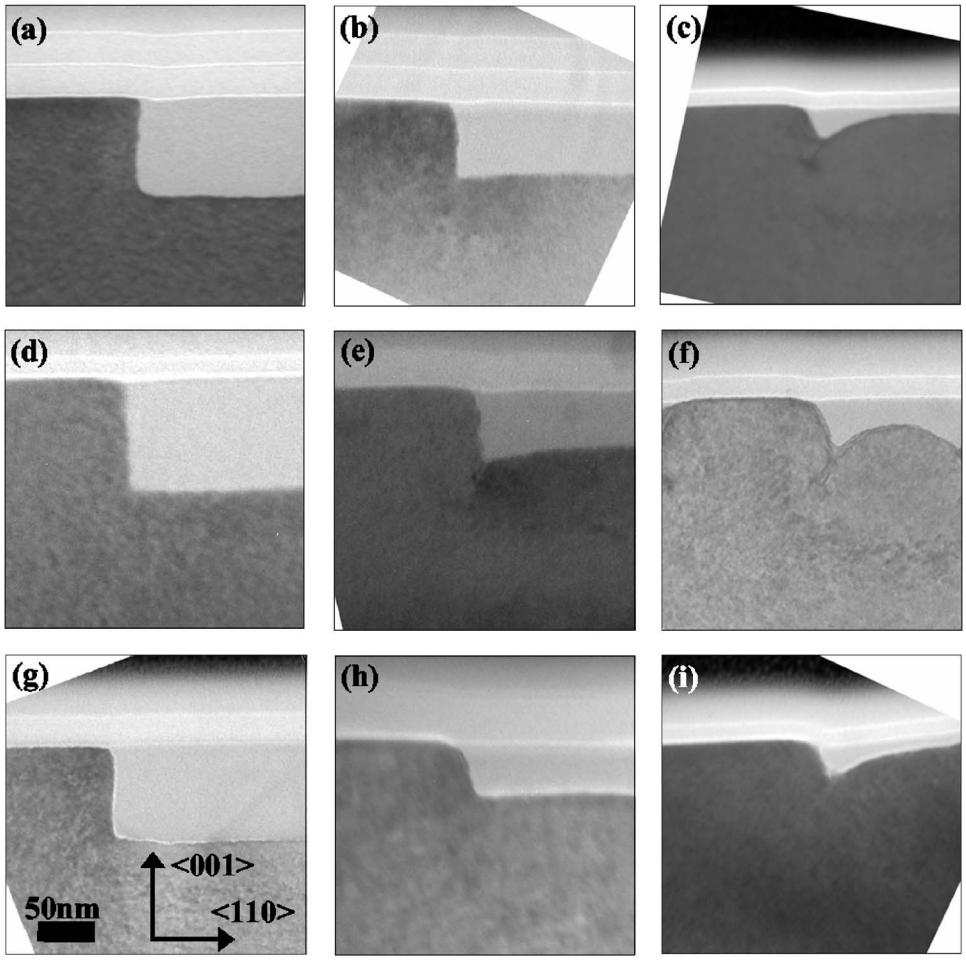

FIG. 2. XTEM micrographs of samples annealed for (a) 1 h, (b) 2 h, and (c) 3 h without stress; (d) 1 h, (e) 2 h, and (f) 3 h under compressive stress of 200 MPa; and (g) 1 h, (h) 2 h, and (i) 3 h under tensile stress of 200 MPa.

times are presented in Figs. 3(a) and 3(b), respectively. As shown in Figs. 3(a) and 3(b), as SPE proceeds for stress-free samples, θ decreases from 90° after 1 h to 76° after 2 h, indicative of the two interface meeting.

Cross-sectional transmission electron microscopy images of samples annealed up to 3 h under a compressive stress of 200 MPa are presented in Figs. 2(d)–2(f). There is little difference compared to the stress-free sample after 1 h of annealing, as shown in Fig. 2(d), and θ shows little variation after 1 h, as shown in Fig. 3(a). However, after 2 h of annealing shown in Fig. 2(e), pinch-off of the interfaces has occurred. After 3 h of annealing, significant defect evolution has occurred, as shown in Fig. 2(f). Compared to the stress-free case, the evolution of the mask edge defect begins earlier in the SPE process at ~2 h of annealing when a compressive stress is applied, which agrees with the prior work of Shin *et al.* where a stress of ~500 MPa was applied.[9,10] This is further supported by Fig. 3(b) as θ has decreased significantly after 2 h of annealing, suggesting impingement of the two interfaces which would cause defect formation.

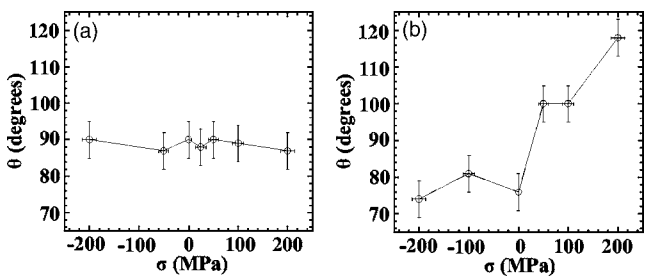

FIG. 3. Plots of θ vs σ for (a) 1 h and (b) 2 h of annealing.

Finally, XTEM images of samples annealed up to 3 h under tensile stress of 200 MPa are presented in Figs. 2(g)–2(i). Once again, the α-Si layer shows little difference compared to compressive or stress-free samples after 1 h of annealing as presented in Fig. 2(g) which is further supported by Fig. 3(a). However, after 2 h of annealing, the corner of the α-Si layer has not started to come to a point or become sharp, suggesting a significant separation of the two interfaces, as displayed in Fig. 2(h). Up to 3 h of annealing, as presented in Fig. 2(i), there is no pinch-off or defect evolution evident in contrast to stress-free and compressive samples. This was observed to be the case for tensile stresses exceeding 100 MPa, consistent with prior research.[3,4] At values of 50 and 25 MPa, defect evolution was evident. Furthermore, in tension θ is much larger than in compression after 2 h of annealing, as shown in Fig. 3(b). The larger values of θ are indicative of greater separation of the regrowth interfaces which presumably prevents mask edge defect formation.

A model is presented here to explain the observations in regrowth and defect formation. Many have revealed an exponential stress dependence of $v_{\langle 001 \rangle}$ for both hydrostatic pressure and uniaxial stress as described elsewhere.[5–7] In these studies, the activation strain for a particular stress state ΔV was introduced and used to describe the response of $v_{\langle 001 \rangle}$ to stress. For a generalized stress state σ_j, where j is

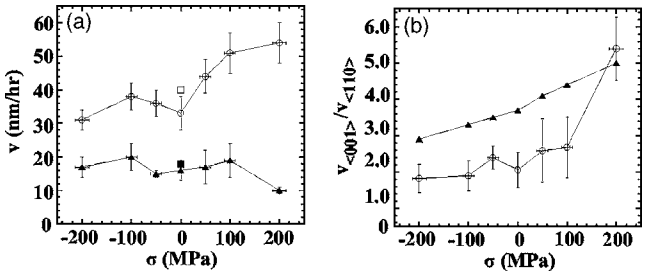

FIG. 4. Plots of (a) $v_{\langle 001\rangle}$ (circles) and $v_{\langle 110\rangle}$ (triangles) vs σ and of (b) $v_{\langle 001\rangle}/v_{\langle 110\rangle}$, observed (circles) and predicted (triangles), versus σ. The open (Ref. 11) and filled (Ref. 12) squares in (a) denote reported values of $v_{\langle 001\rangle}$ and $v_{\langle 110\rangle}$, respectively.

the stress direction, ΔV is taken to be a tensor, ΔV_{ij}, of the form

$$\Delta V_{ij} = \begin{bmatrix} \Delta V_{11} & \Delta V_{12} & \Delta V_{12} \\ \Delta V_{12} & \Delta V_{11} & \Delta V_{12} \\ \Delta V_{12} & \Delta V_{12} & \Delta V_{11} \end{bmatrix}, \tag{1}$$

where i is the regrowth direction. In standard crystal orientation there are two independent terms. The off-diagonal terms are taken to be a value of 0.14 Ω measured experimentally by Barvosa-Carter and Aziz,[5] while the diagonal terms are taken to be a value of -0.58 Ω predicted by Aziz *et al.*,[6] where Ω is the atomic volume of Si of 12 $\mathrm{cm}^3/\mathrm{mol}$. From the values ΔV_{11} and ΔV_{12}, it is evident that stress in the regrowth direction has the greatest influence on regrowth enhancement, while stresses orthogonal to the regrowth direction have significantly smaller effects. Furthermore, the negative value for ΔV_{11} indicates that a compressive normal stress will enhance regrowth, while the positive value of ΔV_{12} suggests that tensile transverse stress will enhance regrowth. The model presented here assumes that the regrowth velocity in the i direction, v_i, for a given crystal orientation obeys the relationship

$$v_i = v_{i0} \exp\left(\frac{\sigma_1' \Delta V_{i1}' + \sigma_2' \Delta V_{i2}' + \sigma_3' \Delta V_{i3}' - \Delta E_i}{kT} \right), \tag{2}$$

where σ_1', σ_2', and σ_3' are the normal stresses and $\Delta V_{i1}'$, $\Delta V_{i2}'$, and $\Delta V_{i3}'$ are the activation strains calculated by transforming σ_j and ΔV_{ij} to the specified orientation, v_{i0} is an orientation-dependent preexponential factor, ΔE_i is the activation energy for SPE in the i direction, k is Boltzmann's constant of 8.62×10^{-5} eV/K, and T is the temperature in Kelvin.

A plot of $v_{\langle 001\rangle}$ and $v_{\langle 110\rangle}$ versus stress is presented in Fig. 4(a) with published values of stress-free bulk regrowth provided for comparison.[11,12] From Fig. 4(a), enhancements to $v_{\langle 001\rangle}$ along with retardation of $v_{\langle 110\rangle}$ in tension are observed. These are predicted by the model. The model also correctly predicts the retardation of $\langle 001\rangle$ regrowth and the enhancement of $\langle 110\rangle$ regrowth in compression.

It is interesting to consider the ratio of $v_{\langle 001\rangle}$ and $v_{\langle 110\rangle}$ versus stress compared to predicted values calculated using Eq. (2) and the data of Csepregi *et al.*,[12] as shown in Fig. 4(b). The observed ratios qualitatively follow the same trend as the predicted ratios, though they are all lower than predicted. This would imply that $v_{\langle 001\rangle}$ was either slower than expected or $v_{\langle 110\rangle}$ was faster than expected. It is also interesting to note that the smallest deviations from prediction occur at the highest magnitudes of stress where the effect on regrowth would be largest. Additionally, it should be noted that ΔV_{11} was not experimentally measured in the study conducted by Aziz *et al.*[6]

It is interesting to note the negative deviations in the measured regrowth velocities relative to published values as well the large negative deviations in $v_{\langle 001\rangle}/v_{\langle 110\rangle}$ relative to predicted values. At lower stresses, small variations in temperature would have a greater effect on the observed velocities. Furthermore, deviations possibly stem from the inherent difficulty in measuring different regrowth velocities within a two-dimensional structure compared to bulk material. Likewise, bowing of the α-Si layer during regrowth, resulting from the interface being pinned at the site of defect formation and at the surface, would presumably slow regrowth. If this effect was greater on $v_{\langle 001\rangle}$ than on $v_{\langle 110\rangle}$, this would explain the negative deviations observed in the velocity ratios.

Most importantly, the trend observed in Fig 4(b) is consistent with the observations of defect evolution. Larger ratios suggest larger separation between the two interfaces along with larger values of θ and, subsequently, suppression of defects. Comparing this to the trends observed with the evolving interface angle with stress, this is exactly what was observed.

We have investigated the effect of uniaxial stress on solid phase epitaxy in patterned Si wafers in an effort to control mask edge defect formation. Cross-sectional transmission electron microscopy of samples annealed up to 3 h under different stresses revealed that compressive and tensile stresses retard and enhance $\langle 001\rangle$ regrowth while enhancing and retarding $\langle 110\rangle$ regrowth, respectively. Furthermore, the evolving interface angle between the $\langle 110\rangle$ and $\langle 001\rangle$ regrowth fronts was observed to increase with increasing tensile stress. Moreover, tensile stresses of 100 MPa or greater were found to suppress defect formation, presumably by preventing the meeting of the two regrowing interfaces. The presented model for stress enhancements to regrowth correctly predicts the observed trend in regrowth velocities and confirms the observed conditions necessary for defect suppression or formation.

The authors wish to acknowledge the Semiconductor Research Corporation for supporting this work.

[1] H. Cerva and K.-H. Kusters, J. Appl. Phys. **66**, 4723 (1989).
[2] H. Cerva, Defect Diffus. Forum **148**, 103 (1997).
[3] C. Ross and K. S. Jones, Mater. Res. Soc. Symp. Proc. **810**, C10.4 (2004).
[4] C. R. Olson, E. Kuryliw, B. E. Jones, and K. S. Jones, J. Vac. Sci. Technol. B **24**, 446 (2006).
[5] W. Barvosa-Carter and M. J. Aziz, Appl. Phys. Lett. **79**, 356 (2001).
[6] M. J. Aziz, P. C. Sabin, and G.-Q. Lu, Phys. Rev. B **44**, 9812 (1991).
[7] E. Nygren, M. J. Aziz, and D. Turnbull, Appl. Phys. Lett. **47**, 232 (1985).
[8] T. K. Chaki, Philos. Mag. Lett. **63**, 303 (1991).
[9] Y. G. Shin, J. Y. Lee, M. H. Park, and H. K. Kang, J. Cryst. Growth **233**, 673 (2001).
[10] Y. G. Shin, J. Y. Lee, M. H. Park, and H. K. Kang, Jpn. J. Appl. Phys., Part 1 **40**, 6192 (2001).
[11] J. M. Poate, S. Coffa, D. C. Jacobson, A. Polman, J. A. Roth, G. L. Olson, S. Roorda, W. Sinke, J. S. Custer, M. O. Thompson, F. Spaepen, and E. Donovan, Nucl. Instrum. Methods Phys. Res. B **B55**, 533 (1991).
[12] L. Csepregi, E. F. Kennedy, and J. W. Mayer, J. Appl. Phys. **49**, 3906 (1978).